

Pro-fibrotic effect of IL-6 via aortic adventitial fibroblasts indicates IL-6 as a treatment target in Takayasu arteritis

X. Kong¹, L. Ma¹, Z. Ji¹, Z. Dong², Z. Zhang³, J. Hou⁴, S. Zhang⁵, L. Ma¹, L. Jiang^{1,6}

¹Department of Rheumatology, and ²Department of Vascular Surgery, Zhongshan Hospital, Fudan University, Shanghai; ³Department of Pathology, Shanghai Medical College, Fudan University, Shanghai; ⁴Department of Pathology, Zhongshan Hospital, Fudan University, Shanghai; ⁵Key Laboratory of Glycoconjugate Research Ministry of Public Health, Gene Research Center, Department of Biochemistry and Molecular Biology, School of Basic Medical Sciences, Fudan University, Shanghai; ⁶Center of Clinical Epidemiology and Evidence-based Medicine, Fudan University, Shanghai, China.

Abstract

Objective

This study aimed to clarify potential mechanism of IL-6 involved in adventitial fibrosis via adventitial fibroblast in Takayasu arteritis (TAK).

Methods

Immunohistochemistry and double-labelled immunofluorescence were performed on vascular tissue from patients with TAK and controls. Human aorta adventitial fibroblast (AAF) was cultured and stimulated with interleukine 6 (IL-6)/IL-6 receptor (IL-6R). Real-time PCR, western blot, enzyme-linked immunosorbent assays, chromatin immunoprecipitation (ChIP) and reporter assay were conducted in vitro experiments to determine effect of IL-6/IL-6R on AAF.

Results

The expression of IL-6, IL-6R, collagen I, collagen III, fibronectin, α -smooth muscle actin (α -SMA), and transforming growth factor (TGF- β) in TAK arteries was significantly higher than that in the normal arteries. Co-localisation of α -SMA and IL-6 and a positive correlation between their expression were observed in local lesions. In vitro experiments, collagen I, collagen III, fibronectin, α -SMA, and TGF- β expression increased significantly after stimulation and this fibrogenesis of AAFs was induced in TGF- β -dependent and -independent manners. Additionally, phosphorylation of JAK2, STAT3 and Akt was significantly enhanced both in IL-6/IL-6R-treated AAFs in vitro and in TAK adventitial α -SMA positive cells. When AAFs were pretreated with inhibitors against JAK2, STAT3, and Akt, fibrosis was significantly reduced. Furthermore, IL-6/IL-6R promoted mRNA expression of IL-6 and MCP-1 in AAFs. Finally, according to ChIP and reporter assay results, STAT3 was the main transcriptional factor in the fibrosis of AAFs induced by IL-6/IL-6R.

Conclusion

IL-6/IL-6R induces fibrogenesis of AAFs via the JAK2/STAT3 and JAK2/Akt pathways, which provides theoretical evidence for IL-6 as a treatment target in TAK.

Key words

Takayasu arteritis, IL-6, vascular fibrosis, adventitial fibroblast

Xiufang Kong, MD, PhD*

Lili Ma, MD, PhD*

Zongfei Ji, MD

Zhihui Dong, MD

Zhigang Zhang, MD

Jun Hou, MD

Si Zhang, PhD

Lingying Ma, MD

Lindi Jiang, MD, PhD

*These authors contributed equally to this work.

Please address correspondence to:

Dr Lin-Di Jiang,

Department of Rheumatology,

Zhongshan Hospital,

Fudan University,

180 Fenglin Road,

200032 Shanghai, China.

E-mail: zsh-rheum@hotmail.com

Received on February 16, 2017; accepted

in revised form on April 18, 2017.

© Copyright CLINICAL AND

EXPERIMENTAL RHEUMATOLOGY 2018.

Introduction

Takayasu arteritis (TAK) is a type of chronic granulomatous vasculitis that involves the aorta or its main branches. It is more common among young females who are <40 years old (1). The prevalence rate of TAK is higher in Southeast Asia countries, with about 40 cases per million reported in Japan and only 4–8 cases per million reported in the rest of the world (2). Although the precise incidence rate of TAK in China is unclear, it has been increasing in recent years.

TAK is a chronic disorder that is characterised by abnormal vascular structure, such as vascular thickness, vascular occlusion or vascular aneurysm. According to epidemiological data of our centre, there are more than 90% of patients with TAK presenting vascular thickness or vascular occlusion due to tissue fibrosis. However, the current therapeutic methods such as prednisone and cyclophosphamid for TAK cannot prevent or treat vascular fibrosis. Thus clarifying mechanism of vascular fibrosis is critical for exploration of new treatment target (3).

Recently, more and more clinical reports demonstrated that biological agent targeted interleukin 6 (IL-6) receptor such as tocilizumab was effective in large-vessel vasculitis, including refractory TAK (4–6). In our previous study, we found that IL-6 receptors were infiltrated in local lesions, especially in adventitia (7). Tamura *et al.* reported that IL-6 was a potent biomarker of disease activity (8). Actually, IL-6 has been reported to promote tissue fibrosis via acting on local fibroblast in many fibrotic disorders, such as cardiac fibrosis and sclerosis (9, 10), but fibroblast has tissue-specific features (11). In TAK, vascular fibrosis started from adventitia, which is composed of a great amount of fibroblasts. Thus, elucidating whether IL-6 has pro-fibrotic effect via adventitial fibroblast in TAK is helpful to explicit the effect of Tocilizumab in TAK. Therefore, the aim of this study was to investigate the pro-fibrotic effects of IL-6 on adventitial fibroblasts and delineate the possible therapeutic mechanism of current biological agent targeted IL-6 in TAK.

Materials and methods

Study population

Fourteen patients with TAK who had undergone surgery were recruited from Zhongshan Hospital, Fudan University from January 1st, 2013 to September 1st, 2016. They were diagnosed according to the American College of Rheumatology 1990 criteria and suggestions of two experienced rheumatologists. General information and clinical characteristics of all patients were collected at the time of disease onset. In addition, specimens of 1 normal aortic and 4 normal renal arteries were obtained from patients who had undergone heart transplant or nephrectomy.

Ethical considerations

The study protocol was approved by the Ethics Committees of Zhongshan Hospital and conforms to the ethical guidelines of the 1975 Declaration of Helsinki. All the patients provided their written informed consent for inclusion in this study.

Immunohistochemistry (IHC)

IHC was performed as previously described (7). In brief, after sections were deparaffinised and rehydrated, antigen retrieval was carried out using citrate buffer solution (0.01 mol/L, pH 6.0). Endogenous peroxidase activity was blocked by 3% H₂O₂. Each slide was blocked with goat serum and incubated for 30 min. Subsequently, slides were incubated with diluted primary antibody for 1 h at 37°C and transferred from the chamber to 4°C overnight. The next day, slides were warmed to room temperature and secondary antibody was added to each slide for 1 h at 37°C. At last, sections were developed with DAB reagent, counterstained with haematoxylin and mounted with neutral gum.

Antibodies of α -smooth muscle actin (α -SMA), collagen I, collagen III, fibronectin, IL-6, IL-6R, transforming growth factor- β (TGF- β), connective tissue growth factor (CTGF), STAT3, p-STAT3 (Y705), Akt, and p-Akt (Ser473) purchased from Abcam, Cambridge, Mass. Serial sections of vascular tissues were used. All slides were scanned with a 3DHISTECH scanner microscope and images were selected

Funding: this work was supported by the National Natural Science Foundation of China (no. 81571571).

Competing interests: none declared.

by Panoramic Viewer 1.15.3. Five 10-fold magnification fields on the viewer were randomly selected. The integrated optical density (IOD) and area of the selected images were determined by the Image Pro plus software v. 3.1 (Media Cybernetics, Silver Spring, USA). Protein expression was presented as the ratio of IOD to the relevant area.

Double-labelled immunofluorescence

The procedures in this experiment were carried out as previously described (12). In short, sections were deparaffinised and rehydrated at first, then antigen retrieval was carried out using EDTA antigen retrieval solution. After that, each slide was blocked with 3% bovine serum albumin (BSA) for 30 min at room temperature. Subsequently, two kinds of diluted antibodies from different species were used to incubate slides for 1 h at 37°C and then 4°C overnight. The next day, slides were incubated with species-specific fluorochrome conjugated secondary antibodies for 1 h at 37°C. At last, slides were counterstained with DAPI reagent and mounted with medium with the function to prevent quenching. Primary antibodies included mouse monoclonal anti- α -SMA (Abcam) and rabbit monoclonal anti-IL-6 antibody (Abcam). The secondary antibodies were Alexa Fluor 488-conjugated goat anti-rabbit and Cy3-conjugated goat anti-mouse antibodies (Beyotime Biotechnology, China). The protein levels in the slides were analysed as mentioned above by Image Pro plus software.

Cell culture

Human aortic adventitial fibroblasts (catalogue no. 6120, AAF) and human skin fibroblasts (HSF) were purchased from Sciencell Research Laboratories (Corte Del Cedro, Carlsbad CA, USA). AAF was cultured in a specific medium (Fibroblast medium, catalogue no. 2301, Sciencell Research Laboratories). HSFs were cultured in Dulbecco's modification of Eagle's medium (DMEM) supplemented with 10% fetal bovine serum. All experiments were performed before passage eight and cells were starved overnight before intervention.

In this study, different concentrations of IL-6/IL-6R (0, 20, 50, 100ng/ml) were used to stimulate AAF and collagen I, collagen III, fibronectin, TGF- β and α -SMA levels were detected at different time point (0, 12, 24, 48, 72 hours) to observe effects of IL-6/IL-6R to AAF. Also, signalling pathway and mechanism involved in this process were explored at different time points (0, 15, 30, 45, 60, 120 min).

Cell proliferation

The proliferation of AAFs was detected after IL-6/IL-6R (R&D, Minneapolis, MN, USA) stimulation (50 ng/ml) using the cell counting kit (Dojindo, Kumamoto, Japan). Absorbance at 450 nm was calculated using FlexStation3 Multi-Mode Microplate Reader (Molecular Devices, USA). Six replicates were performed in each experiment.

RAN isolation and quantitative real-time PCR

RNA was extracted using the Trizol reagent (Invitrogen, Carlsbad, CA, USA) and quantified using spectrophotometry (Denovix DS-11; Denovix, Wilmington, Delaware, USA). The PrimeScript RT reagent kit (RR047A; Takara Biotechnology) and Ex Taq SYBR green premix (RR420A, Takara Biotechnology) were used for reverse transcription and later qualification. The comparative Ct method was used to calculate gene expression.

Western blot (WB)

WB was performed using a previously described method (13). Primary antibodies against collagen I (Abcam), collagen III (Abcam), fibronectin (Abcam), β -tubulin (Abcam), β -actin (Abcam), phospho-Jak2, total Jak2, phospho-Stat3 (Ser727, Tyr705), total-Stat3, phospho-Akt (Thr308, Ser473), total Akt, phospho-ERK1/2 (E4), total ERK 1/2 (K23), phospho-p38, total p-p38, phospho-JNK, and total JNK were used. Antibodies about signal pathway proteins were purchased from Cell Signaling Technology Inc. The secondary antibodies included anti-rabbit IgG (Sigma-Aldrich) and anti-mouse IgG (Sigma-Aldrich). Images were analysed with the Gel pro analyser 4.0.

ELISA assays

The human IL-6 and monocyte chemoattractant protein 1 (MCP-1) ELISA kit (R&D Systems, Minneapolis, MN, USA) was used to detect their levels in the culture medium.

Transient transfection of cells

TGF- β siRNA and FAM-tagged non-target control siRNA (siRNC) was designed (GenePharma). The siRNA sense sequences and control sequences are 5'-CCUGUGACAGCAGG-GAUAATT-3' and 5'-UUCUC-CGAACGUGUCACGUTT-3' separately. The transfection protocol was performed as previously described (13).

Viral particle production

Recombinant lentiviruses were produced by co-transfection of HEK293T cells with the pVSVG, p Δ R, and pLKO.1-puro vectors containing full-length IL-6 ssRNA or irrelevant RNA as the control.

ChIP assay

Transcriptional effect of STAT3, AP1, cyclic AMP (cAMP)-responsive element binding protein (CREB) and CCAAT/enhancer binding protein (C/EBP- β) on collagen I, collagen III and fibronectin was detected by ChIP assay. Antibodies against STAT3 (sc-8019X; Santa Cruz, CA, USA), CREB (Abcam), C/EBP- β (Abcam) and AP-1 (Abcam), or control rabbit IgG (Pepro-Tech) were used.

Construction of luciferase reporter plasmids

The 506-bp collagen I promoter sequences (0 to -506) were PCR amplified from human genomic DNA using the relevant primers (Table I). The PCR products were then digested with *KpnI*/*NheI* and inserted into luciferase reporter plasmid pGL3-Basic (Promega, Fitchburg, WI, USA) to generate collagen I (WT) Luc. The forward and reverse primers used to generate the collagen I (mSTAT3) Luc vector that contains the same collagen I promoter sequences but with mutations that distort the STAT3 consensus are listed in Table I. The PCR products were again digested with *KpnI*/*NheI* and ligated into pGL3-Basic.

Table I. Primers used in construction of luciferase reporter plasmids.

Gene	Primers	Sequences
Collagen I promoter	Forward	CTATCGATAGGTACCTCCCCAGTTCCTCCAC
	Reverse	CTATCG ATA GGTACCTCCCCA GTTCCCCAGTTCAC
Collagen I (mSTAT3)	Forward	GCTGCCCTCCCAGAGCTGCGAAGAGGGG
	Reverse	TCTGGGAGGGCAGCCCCCAGCCAGCC

Transfection and reporter assay

Collagen I promoter (collagen I WT: 0~506 bp, collagen I with mutation: 0~500bp, which inhibited the binding site for STAT3) with upstream of the luciferase gene was constructed. In collagen I with mutation promoter, STAT3 binding site (-325 GGGAGG -318) was mutated into (-325 CCCTCC -318). HSF were then transfected with the pRL-TK plasmid containing collagen I (WT) or collagen I (mSTAT3) using the liposome-mediated method with the Lipofectamine 2000 reagent (Invitrogen). Luciferase activity was measured using a dual-luciferase reporter assay system (Promega).

Statistical analysis

Data regarding patients' characteristics was expressed as the mean ± SD values, and results of western blot were expressed by mean ± SEM and analysed by two-way ANOVA or the Student *t*-test. Pearson correlation analysis was also performed. All statistical analyses were performed using SPSS v.

20.0 (Chicago, IL, USA). Histograms were generated using Graphpad prism 5 (GraphPad Software Inc., USA). *P*-values <0.05 were considered to indicate statistically significant differences.

Results

Patient characteristics

Fourteen patients (8 female and 6 male) with TAK were recruited in this study (age, 38.28±13.5 years). Their IL-6 levels (21.62±21.3 pg/ml) were higher than normal levels. Detailed characteristics were listed in Table II.

Excess ECM deposition in TAK-involved arteries

The expression of IL-6, IL-6R, α-SMA, ECM proteins (collagen I, collagen III and fibronectin), TGF-β and CTGF was significantly higher in the vascular adventitia of patients with TAK than in the normal arteries (*p*<0.05, Fig. 1A and C). Double-labelled fluorescence staining displayed co-localisation of IL-6 and α-SMA (Fig. 1B). Correlation analysis indicated a positive correla-

tion between the expression of IL-6 and α-SMA in the TAK arteries (*p*<0.05, *R*² = 0.89, Fig. 1D).

Increased fibrogenesis in AAFs induced by IL-6/IL-6R in TGF-β-dependent and -independent manners

Our preliminary data indicated that the IL-6/IL-6R signalling pathway in AAFs can be potently activated at an IL-6/IL-6R dose of 50 ng/ml with a ratio 1:1. A striking increase in the proliferation of AAFs was observed after IL-6/IL-6R stimulation (Supplementary Fig. 1A-C. Expression of α-SMA, collagen I, collagen III, fibronectin and TGF-β (total form) reached its peak at different time points (72 h for α-SMA and fibronectin and 8 h for collagen I, collagen III and TGF-β). The expression of α-SMA, collagen III and TGF-β was enhanced in a concentration-dependent manner (Fig. 2 C and D), while the expression of collagen I and fibronectin peaked at 20 ng/ml. However, no increase in CTGF expression was detected in AAFs at any concentration.

After the AAFs were transfected with the IL-6 overexpression vector, increase in fibrogenesis was also observed (Fig. 2 E and F). On the other hand, when AAFs was pretreated with TGF-β siRNA (*p*<0.05, Fig. 2 G and H), the expression of collagen I and colla-

Table II. Patient characteristics.

No	Sex	Age at onset (years)	Disease duration (months)	Kerr	ESR (mm/H)	CRP (mg/L)	IL-6 (pg/ml)	Imaging type	Specimen	Reason for surgical treatment	Current treatment*
1	F	46	18	2	40	17	4.4	V	AA	Hypertension	L 10mg qd + P 5mg qd
2	M	31	12	3	120	89	48.2	Ila	AA	Aortic aneurysm	T 25mg qd + P 15mg qd
3	M	42	1	1	36	2.6	5.1	Ila	AV	Aortic regurgitation	HCQ 100mg bid + P 20mg qd
4	F	31	228	2	15	3.5	2.94	V	AA	Aortic regurgitation	T 25mg bid + P 16mg qd
5	F	58	36	3	112	33	2	III	AA	Aortic regurgitation	HCQ 100mg bid + P 8mg qd
6	M	42	8	2	71.4	80	13.4	Ila	AA	Aortic regurgitation	P 20mg qd + T 50mg qn
7	M	56	1	2	22	25	34.1	Ila	AV	Aortic regurgitation	M 12.5mg bid
8	M	40	24	3	68	33	23	Ila	AV	Aortic regurgitation	P 10mg bid + MMF 0.5g bid
9	F	26	12	3	39	0.4	8.33	V	AB	Abdominal aortic aneurysm	P 10mg qd + HCQ 100mg bid + MTX 10mg qw
10	F	20	13	2	10	0.9	10.5	III	AA	Hypertension	P 2.5mg qd + HCQ 100mg bid
11	M	41	1	2	61	22	18.7	Ila	AV	Aortic regurgitation	T 25mg tid + P 10mg bid
12	F	25	312	2	11	38	74.1	Ila	AV	Aortic regurgitation	M 12.5 bid
13	F	19	1	3	39	16	44.6	III	RA	Hypertension	P 30mg qd
14	F	59	12	4	94	67	13.3	V	AV	Aortic regurgitation	P 15mg qd + L 10mg qd

F: female; M: male; AA: aorta; AV: aortic valve; AB: abdominal aorta; RA: renal artery; L: leflunomide; P: prednisone; T: thalidomide; HCQ: hydroxychloroquine; M: metoprolol; MMF: mycophenolate mofetil; MTX: methotrexate.

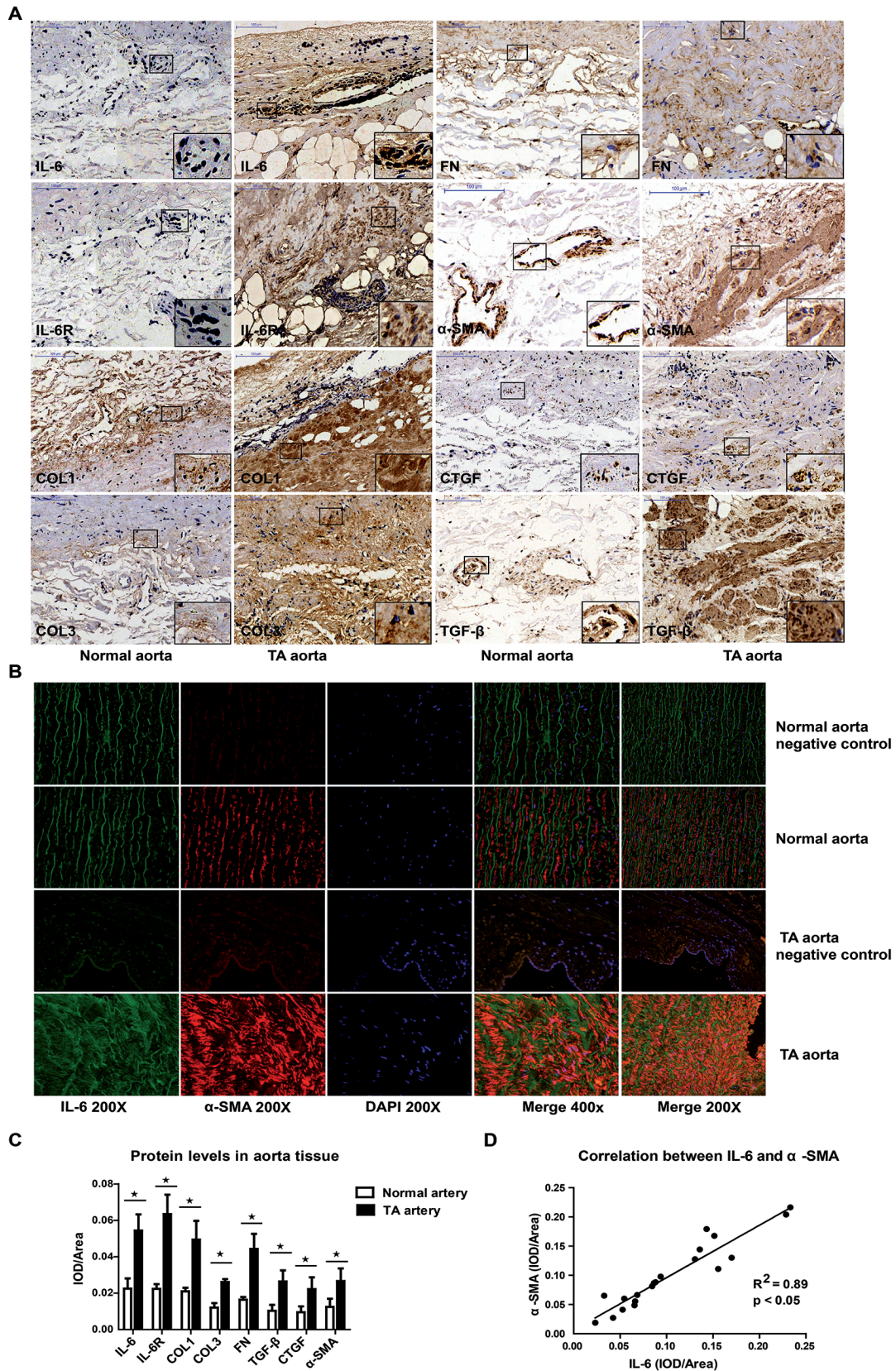


Fig. 1. Increase in ECM deposition and co-localisation of IL-6 and α -SMA in the adventitia in TAK
A: Representative IHC images of various proteins, including IL-6, IL-6R, collagen I, collagen III, fibronectin, CTGF, TGF- β and α -SMA, are shown.
B: Representative double-labelled immunofluorescence images of IL-6 and α -SMA are shown (200 \times and 400 \times).
C: Comparison of the relative expression of proteins in TA and normal tissue (n=19).
D: Correlation analysis of the expression of IL-6 and α -SMA (n=19). * p <0.05.

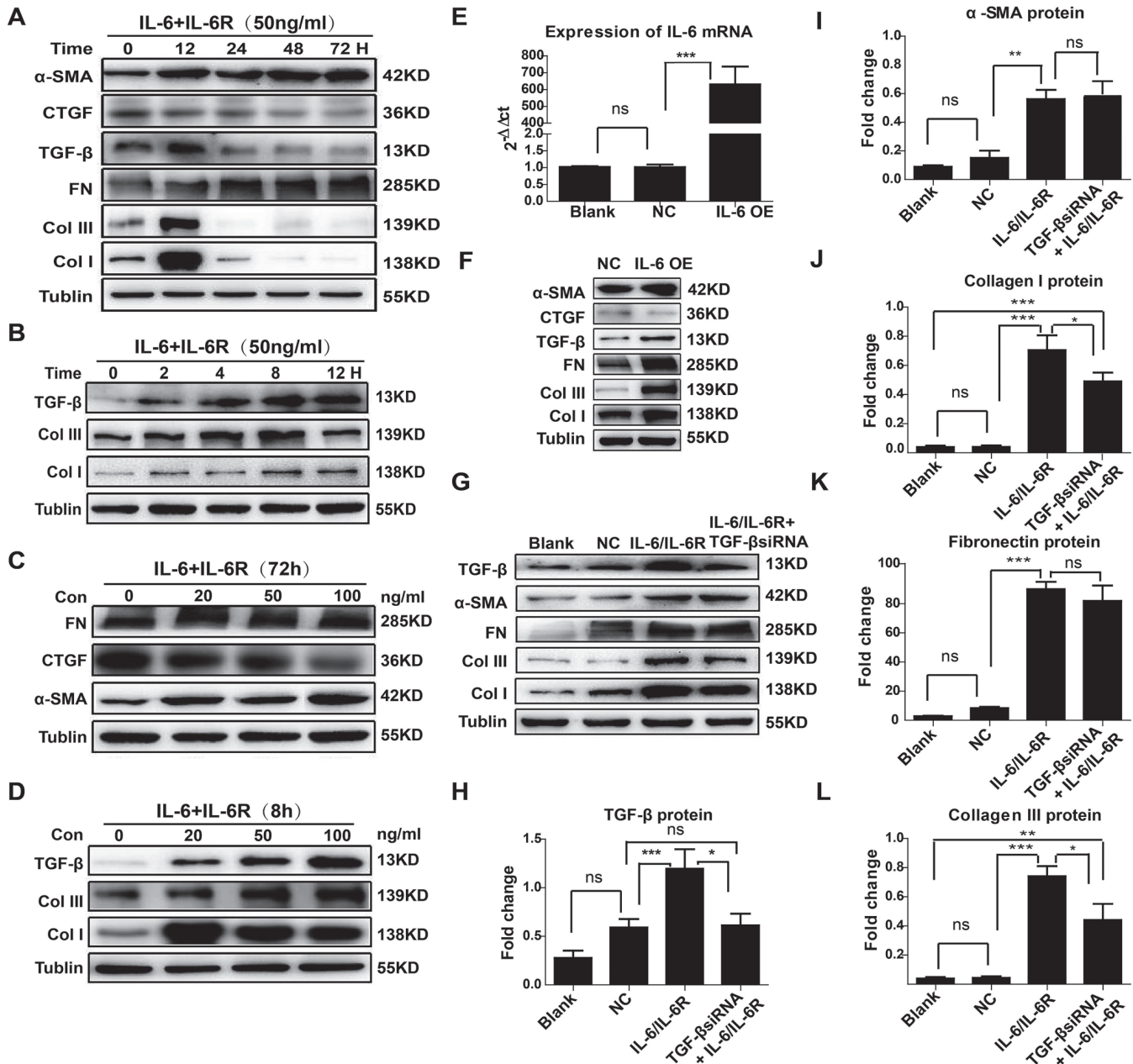


Fig. 2. IL-6/IL-6R-induced increase in fibrogenesis in AAFs and the role of TGF-β. **A:** Representative immunoblots of the expression of proteins, including collagen I, collagen III, fibronectin, CTGF, TGF-β and α-SMA, at 0, 12, 24, 48 and 72 h after IL-6/IL-6R (50 ng/ml) stimulation in AAFs. **B:** Representative immunoblots of collagen I, collagen III and TGF-β expression at 0, 2, 4, 8, and 12 h after IL-6/IL-6R stimulation. **C-D:** Representative immunoblots of the expression of the above proteins at 72/8 h after stimulation with different IL-6/IL-6R concentrations (0, 20, 50, and 100 ng/ml). **E:** Relative mRNA expression of IL-6 in AAFs 24 h after transfection of the IL-6 virus vector. **F:** Representative immunoblots of the expression of the above proteins at 48 h after transfection of the IL-6 virus vector. **G:** Representative immunoblots of the expression of collagen I, collagen III, fibronectin, TGF-β and α-SMA at 48 h after TGF-β siRNA transfection. **H-L:** Densitometric analysis of TGF-β, α-SMA, fibronectin, collagen I and collagen III. The results are expressed as the mean ± SEM values from 3–6 experiments. **p*<0.05, ***p*<0.01, ****p*<0.001.

gen III other than α-SMA and fibronectin in TGF-β siRNA/IL-6/IL-6R group was significantly lower than that in IL-6/IL-6R stimulated group (*p*>0.05, Fig. 2 I-L). However, the levels of collagen I and collagen III in the TGF-β siRNA/IL-6/IL-6R group were still significantly higher than those in the blank group. Thus, IL-6/IL-6R induced fibro-

genesis of AAF partially by a TGF-β-dependent way and partially in a TGF-β-independent manner.

IL-6/IL-6R induced fibrogenesis in AAFs via the JAK2/STAT3 and JAK2/Akt pathways

After IL-6/IL-6R stimulation, phosphorylation of JAK2, STAT3 and Akt

was markedly increased in AAFs (Fig. 3A). When AAFs were pretreated with the JAK2 inhibitor (AG490), phosphorylation of STAT3 and Akt was significantly reduced (*p*<0.05, Fig. 3A-E). Moreover, phosphorylation of STAT3 (Y705) and Akt (Ser473) was also reduced in the presence of the Akt inhibitor (LY294002) or STAT3 in-

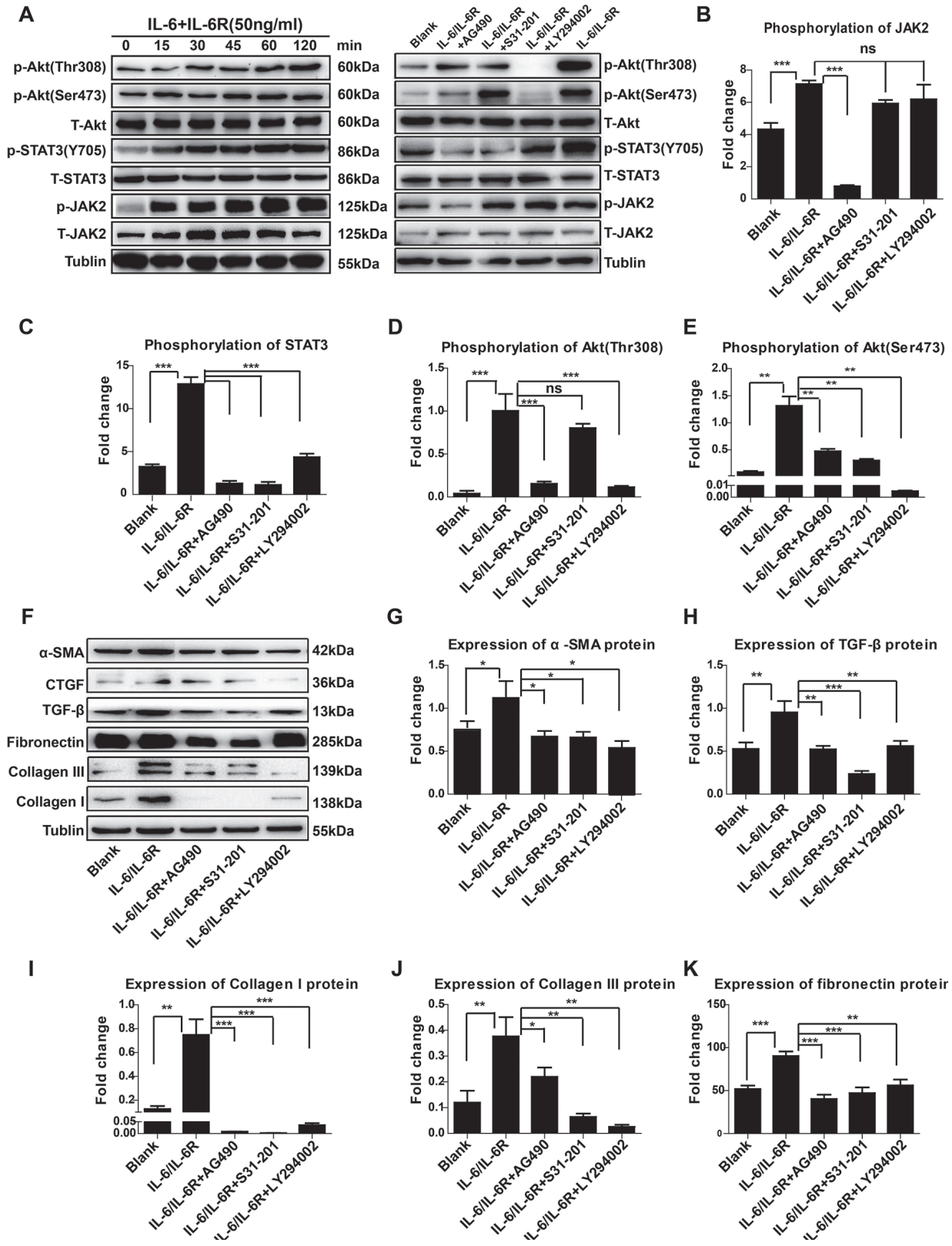


Fig. 3. IL-6/IL-6R-induced fibrogenesis in AAFs via the JAK2/STAT3 and JAK2/Akt pathways. **A:** Representative immunoblots of p-Akt (Thr308), p-Akt (Ser473), p-STAT3 (Y705) and p-JAK2 phosphorylation at 0, 15, 30, 45, 60, and 120 min after IL-6/IL-6R stimulation and their phosphorylation in AAFs 30 min after treatment with IL-6/IL-6R alone or IL-6/IL-6R combined with different inhibitors. **B-E:** Densitometric analysis of phosphorylation of the above-mentioned proteins. The values shown are the ratio of the grey value of the phosphorylated protein to that of the total protein. Results are expressed as the mean \pm SEM values from 3–6 experiments. **F:** Representative immunoblots of the expression of collagen I, collagen III, fibronectin, CTGF, TGF- β and α -SMA at 48 h in the AAFs from different groups. **G-K:** Densitometric analysis of the above mentioned proteins. The results shown are the mean \pm SEM values of 3–6 experiments. * $p < 0.05$, ** $p < 0.01$, *** $p < 0.001$.

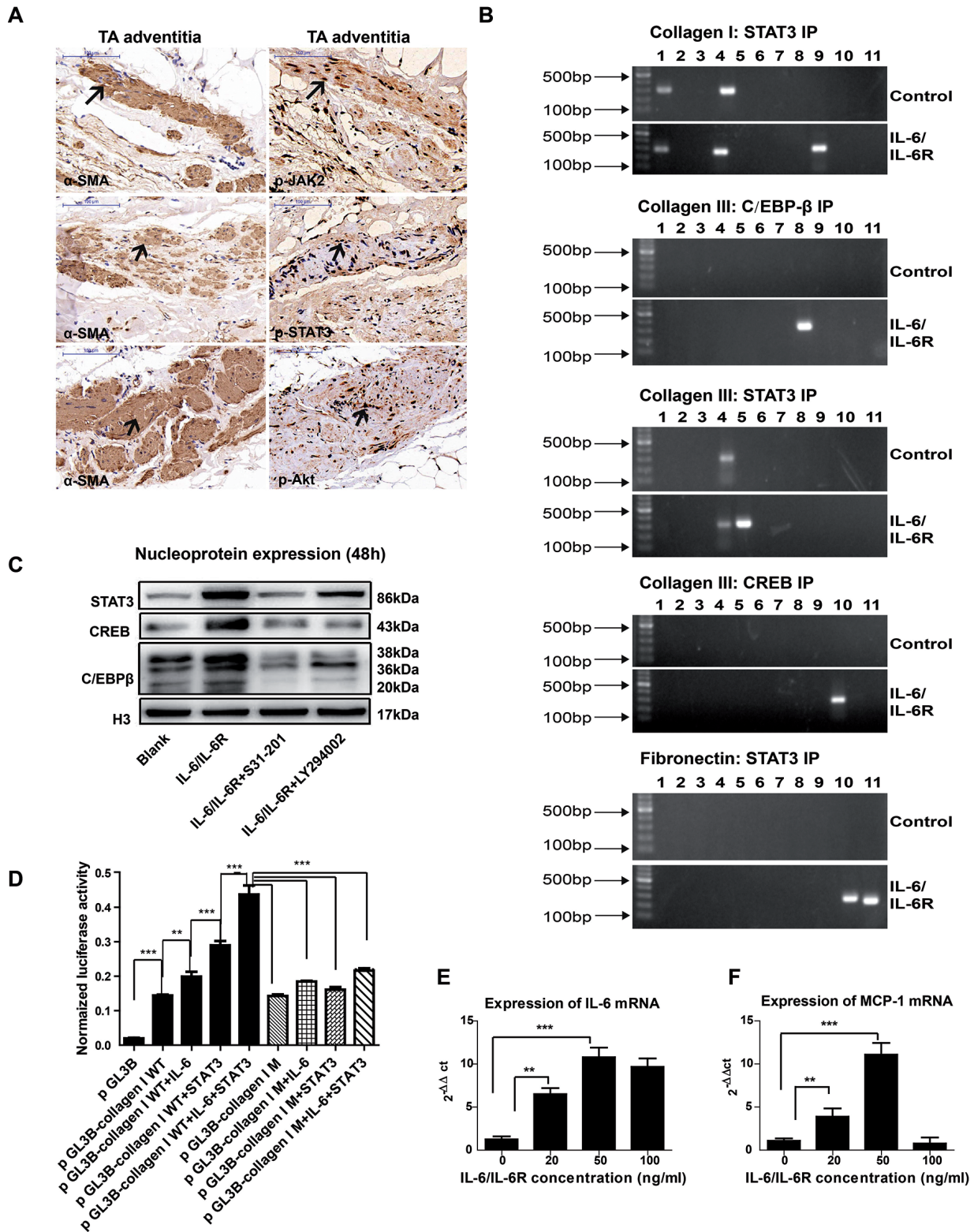


Fig. 4. Activation of JAK2, STAT3 and Akt in local lesions and enhanced transcriptional activity of STAT3, CREB and C/EBP-β and autocrine IL-6 in AAFs. **A:** Representative IHC images of α-SMA positive cells in adventitia and the phosphorylated forms of JAK2, STAT3 and Akt at the corresponding site of α-SMA positive cells in vascular adventitia of patients with TA (Arrows indicated positive staining. Images of phosphorylated signal proteins were selected from the same site with relative images of α-SMA). **B:** ChIP results. Increased STAT3 bound to upstream DNA sequences of promoters of all three proteins, while enhanced CREB and C/EBP-β bound to the promoter of collagen III. **C:** Representative immunoblots of the expression of STAT3, CREB and C/EBP-β in the nucleus at 48 h after treatment with IL-6/IL-6R alone or IL-6/IL-6R combined with the STAT3/Akt inhibitors. **D:** Normalised luciferase activity in different groups. Both the IL-6/IL-6R and STAT3 overexpression plasmids significantly enhanced collagen I WT promoter activity. **E-F:** Expression of IL-6 mRNA and proteins in AAFs at 0, 2, 4, 8, 12, and 24 h after IL-6/IL-6R (50 ng/ml) stimulation. **E-F:** Expression of IL-6 and MCP-1 mRNA in AAFs 24h after IL-6/IL-6R (0, 20, 50, 100ng/ml) stimulation.

hibitor (S31-201) ($p < 0.05$, Fig. 3A-E). Phosphorylation of ERK1/2, p38, JNK and SMAD3 was not obvious in this study (Supplementary Fig. 1D). Levels of α -SMA, collagen I, collagen III, fibronectin, and TGF- β were significantly reduced in AAFs pretreated with the JAK2 or STAT3 inhibitor (Fig. 3F-K). Similarly, the levels of these proteins, except for fibronectin, also decreased in AAFs pretreated with Akt inhibitor. Furthermore, phosphorylation of JAK2, STAT3 and Akt was observed in the vascular adventitial α -SMA positive cells of patients with TAK (Fig. 4A). Based on these results, it was concluded that IL-6/IL-6R induced fibrogenesis in AAFs via the JAK2/STAT3 and JAK2/Akt pathways.

Effect of IL-6/IL-6R on the transcriptional activity of STAT3, CREB and C/EBP- β in AAFs

The ChIP results showed that STAT3 bound to upstream DNA sequences of the promoters of all three proteins, namely, collagen I, collagen III and fibronectin, while CREB and C/EBP- β bound to the promoter of collagen III (Table III, Fig. 4B). The nuclear protein levels of STAT3, CREB and C/EBP- β also significantly increased after IL-6/IL-6R stimulation and decreased in the presence of the STAT3 and Akt inhibitors (Fig. 4C, Supplementary Fig. 1E). In the luciferase reporter assay, collagen I WT promoter activity was significantly increased in the presence of both the IL-6/IL-6R and STAT3 overexpression plasmid but remarkably decreased when fibroblasts were transfected with the collagen I mutant promoter (Fig. 4D).

Elevated IL-6 and MCP-1 mRNA expression in AAFs induced by IL-6/IL-6R

The IL-6 mRNA level increased from 2 h after IL-6/IL-6R stimulation ($p < 0.05$, Supplementary Fig. 1F). The mRNA and protein levels of IL-6 were the highest with the 50 ng/ml IL-6/IL-6R concentration ($p < 0.05$, Fig. 4E, Supplementary Fig. 1G). Moreover, IL-6/IL-6R also induced an increase in MCP-1 mRNA expression in the AAFs (Fig. 4F).

Table III. Regulation of collagen I, collagen III and fibronectin expression by different transcriptional factors.

Gene	Binding site	Primer number	Transcription factor
Collagen I	-485 to -316	9	STAT3
Collagen III	-317 to -91	10	CREB
	-912 to -962	8	C/EBP- β
	-1774 to -1513	5	STAT3
Fibronectin	-503 to -205	10	STAT3
	-774 to -503	11	STAT3

Discussion

The present study presents evidence for the role of IL-6 in the fibrosis of vascular adventitial fibroblasts in TAK and the underlying mechanisms. Overall, the findings indicate that (1) IL-6 does enhance fibrosis in vascular adventitial fibroblasts; (2) Increased fibrogenesis in AAFs is induced by IL-6/IL-6R in TGF- β -dependent and -independent manners; (3) the effects of IL-6 may be mediated via the JAK2/STAT3 and JAK2/Akt pathways; (4) the mechanism may also involve an increase in the transcriptional activity of STAT3, CREB and C/EBP- β ; and (5) IL-6 also promote expressions of IL-6 and MCP-1 in AAFs.

Vascular adventitial fibrosis is known to be a predominant feature of the involved arteries in TAK. Higher expression of collagen I, collagen III, fibronectin and pro-fibrotic factors (TGF- β and CTGF) in the vascular adventitial layer was detected in this study. Higher expression of α -SMA in adventitia represents an increase of myofibroblast cells in vascular lesions. However, myofibroblast cells can derived from multiple cells including fibroblast, smooth muscle cell endothelial cells and resident progenitor cells (11). As sentinel cells of vascular tissue, adventitial fibroblasts were abundant in adventitial layer and easily activated, it was possible that a large proportion of the α -SMA expressing cells were derived from local fibroblasts. As IL-6 is a profibrotic factor, co-localisation of IL-6 and α -SMA and a positive correlation between their expression imply that IL-6 plays an important role in AAF transformation and subsequent fibrosis.

In local lesions, multiple inflammatory cells, such as macrophages, neutrophils and lymphocytes were activated, which

were important sources of IL-6 and soluble IL-6R. Increase in IL-6 and IL-6R expression in local lesions is indicative of the activation of the IL-6 signalling pathway. *In vitro* studies, data indicated that IL-6/IL-6R was capable of inducing phenotypic transformation of AAFs and secretion of more ECM proteins. Additionally, in the present study, the role of TGF- β was investigated, because it has been reported that IL-6 promotes myocardial fibrosis via the TGF- β pathway (14). Our data indicate that TGF- β mediates fibrogenesis of AAF induced by IL-6/IL-6R partially, because not all increased proteins induced by IL-6/IL-6R reduced after TGF- β siRNA intervention. We did not find that IL-6/IL-6R was able to induce CTGF expression *in vitro*, which implied that maybe some other factors in TAK local lesions caused elevation of CTGF.

Very few studies have reported the molecular mechanism underlying vascular fibrosis in TAK. In our study, activation of the JAK2/STAT3 and JAK2/Akt pathways were found not only in AAFs induced by IL-6/IL-6R but also in the vascular adventitial α -SMA positive cells of patients with TAK. In addition, we found that there was an interaction between STAT3 and Akt activation due to their mutual impacts when AAFs were treated with either of both inhibitors. Previous studies have also confirmed that STAT3 and Akt mediated tissue fibrosis. For example, Le *et al.* suggested that blockade of IL-6 transsignalling reduced STAT3 activation and attenuated pulmonary fibrosis (15). Kral *et al.* reported that sustained PI3K activation exacerbated BLM-induced lung fibrosis (16). However, they did not report the mutual effect between STAT3 and Akt.

On the other hand, Erk was also re-

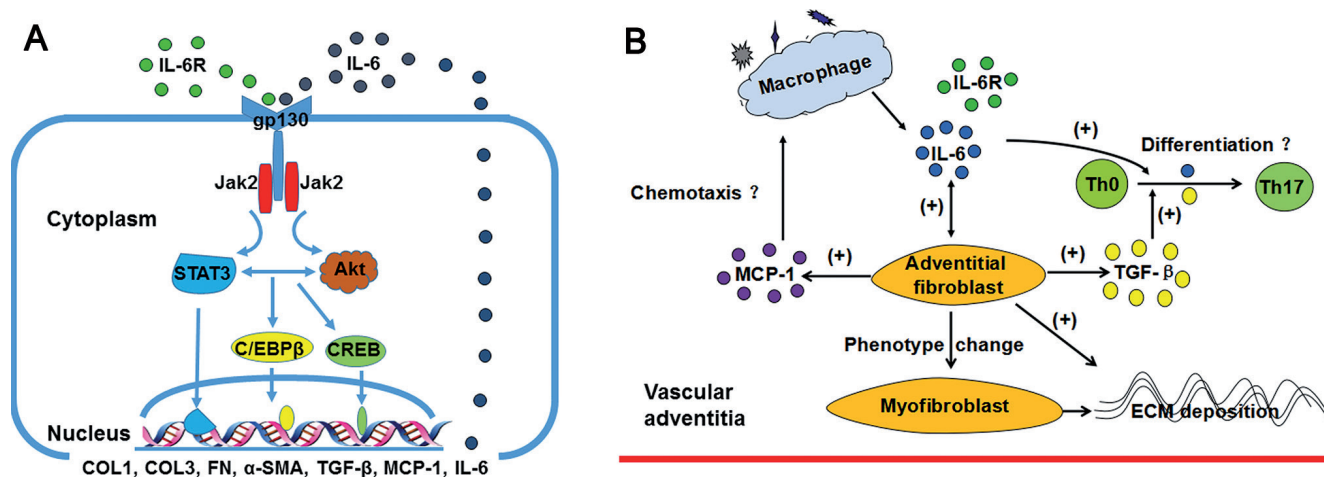


Fig. 5. A cellular model illustrating the mechanisms involved in AAFs after IL-6/IL-6R stimulation. **(B)** A model showing the role of IL-6 in the pathogenesis of TAK via its effects on adventitial fibroblasts. **A:** Specific mechanism about effect of IL-6/IL-6R on adventitial fibroblast: after combining with soluble IL-6R and membrane gp130, the JAK2/STAT3 and JAK2/Akt pathways in the cytoplasm are activated, then the downstream C/EBP β and CREB are stimulated to translocate into the nucleus along with STAT3. Finally, these transcriptional factors bind to promoters of collagen I, collagen III and fibronectin to promote their transcription. **B:** Potential role of IL-6 in TA via adventitial fibroblast: (1) IL-6/IL-6R promotes adventitial fibroblast phenotype transformation and to produce more ECM, which lead to severe fibrosis in local lesions of TA. (2) IL-6/IL-6R enhances adventitial fibroblast to secrete MCP-1, which can recruit more macrophages in situ. Macrophages are important inflammatory cells infiltrated in vascular tissue of TA. (3) Together with TGF- β , IL-6 can induce naive T cells differentiate into Th17 subset, which is another group of inflammatory cells infiltrated in local lesions. (4) IL-6/IL-6R stimulates fibroblast to express more IL-6, which make it a vicious circle as concerned with above three mechanisms. Macrophage is an important source of excess IL-6 and IL-6R at the initial stage.

ported to play a role in tissue fibrosis (17), but our findings did not show this. What is more, O'Reilly *et al.* found that IL-6 trans-signalling drives a STAT3-dependent pathway that leads to hyperactive TGF- β signalling and promotion of SMAD3 activation and fibrosis in dermal fibroblasts (18). However, in our study, although TGF- β was secreted in AAFs after IL-6/IL-6R stimulation, SMAD3 phosphorylation was not observed. Different tissue samples derived fibroblast may explain this distinction. STAT3, C/EBP- β and CREB are transcriptional factors that play a role in fibrogenesis in AAFs, and STAT3 is the most critical one. CREB is currently regarded as a multifaceted protein that is associated with cell survival, proliferation and angiogenesis and can be regulated by growth factors and various cytokines (19, 20). C/EBP- β is also a factor that has a wide array of biologic activities, especially those that involve low-grade inflammation (21). As a chronic vasculitis, fibroblast proliferation, neoangiogenesis and low-grade inflammation all play important role in the pathogenesis of TAK, so STAT3, CREB and C/EBP- β probably involved in this mechanism.

In this study, we also found that IL-6 sustains the inflammatory state of vas-

cular lesions by promoting the secretion of IL-6 from AAFs. C/EBP- β is an important transcriptional regulator of IL-6 expression (22), which may elucidate the overexpression of IL-6 in this study. However, the specific mechanism underlying this effect should be explored further. On the other hand, IL-6 also induced the expression of MCP-1 in AAFs, which would result in the recruitment of more macrophages to vascular lesions. In addition, TGF- β and IL-6 have been reported to be critical factors for Th17 cell polarisation, which is probably an important contributor to the survival of Th17 cells in the vascular tissue of TAK (23, 24). All these findings indicate that the effects of IL-6 are two-fold, that is, it induces fibrosis and inflammation in the micro-environment.

Together with previous reports, we developed a model to illustrate the pathway involved in IL-6/IL-6R mediated adventitial fibroblast fibrosis (Fig. 5A) and this mechanism in the pathogenesis of TAK (Fig. 5B). However, there were several limitations in this study. One of them is that it was impossible to obtain AAFs from patients with TAK because very few patients had undergone surgical treatment and, therefore, there were not enough specimens. In

addition, since no animal model of TAK has been established, these conclusions cannot be verified in animal models. Perhaps these findings can be verified if any animal model of TAK is established in the future.

In conclusion, TAK is a vascular fibrotic disorder in which IL-6 plays a crucial role by enhancing AAF proliferation and inducing phenotypic transformation by increasing ECM secretion via the JAK2/STAT3 and JAK2/Akt pathways. Therefore, treatment strategy that target IL-6 is promising in TAK treatment.

Acknowledgements

We thank Ningli Li for her technical support in this study.

References

- SHARMA BK, S JAIN, S SURI *et al.*: Diagnostic criteria for Takayasu arteritis. *Int J Cardiol* 1996; 54 (Suppl.): S141-7.
- SERRA R, BUTRICO L, FUGETTO F *et al.*: Updates in pathophysiology, diagnosis and management of Takayasu arteritis. *Ann Vasc Surg* 2016; 35: 210-25.
- VAIDEESWAR P, DESHPANDE JR: Pathology of Takayasu arteritis: A brief review. *Ann Pediatr Cardiol* 2013; 6: 52-58.
- OHIGASHI H, TAMURA N, EBANA Y *et al.*: Effects of immunosuppressive and biological agents on refractory Takayasu arteritis patients unresponsive to glucocorticoid treatment. *J Cardiol* 2016; S0914-5087: 30156-3.

5. LORICERA J, BLANCO R, HERNANDEZ JL *et al.*: Tocilizumab in patients with Takayasu arteritis: a retrospective study and literature review. *Clin Exp Rheumatol* 2016; 34 (Suppl. 97): S44-53.
6. KOSTER MJ, MATTESON EL, WAMINGTON KJ: Recent advances in the clinical management of giant cell arteritis and Takayasu arteritis. *Curr Opin Rheumatol* 2016; 28: 211-7.
7. KONG X, SUN Y, MAL *et al.*: The critical role of IL-6 in the pathogenesis of Takayasu arteritis. *Clin Exp Rheumatol* 2016; 34 (Suppl. 97): S21-7.
8. TAMURA N, MAEJIMA Y, TEZUKA D *et al.*: Profiles of serum cytokine levels in Takayasu arteritis patients: Potential utility as biomarkers for monitoring disease activity. *J Cardiol* 2016; pii: S0914-5087: 30291-X.
9. PRELE CM, YAO E, O'DONOGHUE RJ *et al.*: STAT3: a central mediator of pulmonary fibrosis? *Proc Am Thorac Soc* 2012; 9: 177-82.
10. MATSUI F, MELDRUM KK: The role of the Janus kinase family/signal transducer and activator of transcription signaling pathway in fibrotic renal disease. *J Surg Res* 2012; 178: 339-45.
11. STENMAR KR, YEAGER ME, EL KASMI KC *et al.*: The adventitia: essential regulator of vascular wall structure and function. *Annu Rev Physiol* 2013; 75: 23-47.
12. LI C, INESS A, YOON J *et al.*: Noncanonical STAT3 activation regulates excess TGF- β 1 and collagen I expression in muscle of stricturing Crohn's disease. *J Immunol* 2015; 194: 3422-31.
13. ZHU X, XIAO L, HUO R *et al.*: Cyr61 is involved in neutrophil infiltration in joints by inducing IL-8 production by fibroblast-like synoviocytes in rheumatoid arthritis. *Arthritis Res Ther* 2013; 15: R187.
14. WANG JH, ZHAO L, PAN X *et al.*: Hypoxia-stimulated cardiac fibroblast production of IL-6 promotes myocardial fibrosis via the TGF- β 1 signaling pathway. *Lab Invest* 2016; 96: 839-52.
15. LE TT, KANMOUTY-QUINTANA H, MELICOFF E *et al.*: Blockade of IL-6 Trans signaling attenuates pulmonary fibrosis. *J Immunol* 2014; 193: 3755-68.
16. KRAL JB, KUTTKE M, SCHROTTMAIER WC *et al.*: Sustained PI3K activation exacerbates BLM-induced lung fibrosis via activation of pro-inflammatory and pro-fibrotic pathways. *Sci Rep* 2016; 6: 230-34.
17. SAITO F, TASAKA S, INOUE K *et al.*: Role of interleukin-6 in bleomycin-induced lung inflammatory changes in mice. *Am J Respir Cell Mol Biol* 2008; 38: 566-71.
18. O'REILLY S, CIECHOMSKA M, CANT R *et al.*: Interleukin-6 (IL-6) trans signaling drives a STAT3-dependent pathway that leads to hyperactive transforming growth factor- β (TGF- β) signaling promoting SMAD3 activation and fibrosis via Gremlin protein. *J Biol Chem* 2014; 289: 9952-60.
19. STEVEN A, SELIGER B: Control of CREB expression in tumors: from molecular mechanisms and signal transduction pathways to therapeutic target. *Oncotarget* 2016; 7: 35454-65.
20. JOHANNESSEN M, MOENS U: Multisite phosphorylation of the cAMP response element-binding protein (CREB) by a diversity of protein kinases. *Front Biosci* 2007; 12: 1814-32.
21. VAN DER KRIEKEN SE, POPEIJUS HE, MENSINK RP *et al.*: CCAAT/enhancer binding protein β in relation to ER stress, inflammation, and metabolic disturbances. *Biomed Res Int* 2015; 2015: 324815.
22. HUNGNESS ES, LUO GJ, PRITTS TA *et al.*: Transcription factors C/EBP- β and - δ regulate IL-6 production in IL-1 β -stimulated human erythrocytes. *J Cell Physiol* 2002; 192: 64-70.
23. LIU HP, CAO AT, FENG T *et al.*: TGF- β converts Th1 cells into Th17 cells through stimulation of Runx1 expression. *Eur J Immunol* 2015; 45: 1010-8.
24. GEGINAT J, PARONI M, KASTIRR I *et al.*: Reverse plasticity: TGF- β and IL-6 induce Th1-to-Th17-cell transdifferentiation in the gut. *Eur J Immunol* 2016; 46: 2306-10.